

Reduction of carbon footprint from spark ignition power facilities by the dual approach

KATARZYNA JANUSZ-SZYMAŃSKA*
KRZYSZTOF GRZYWNOWICZ
GRZEGORZ WICIAK
LESZEK REMIORZ

Silesian University of Technology, Faculty of Energy and Environmental Engineering, Akademicka 2A, 44-100 Gliwice, Poland

Abstract Power generation units, suitable for individual users and small scale applications, are mainly based on spark ignition engines. In recently performed research, reductions of emissions coming from such units, especially considering carbon dioxide emissions, are deemed as the issue of particular importance. One of solutions, postponed to reduce impact of spark ignition engine-based units on the natural environment, is transition from fossil fuels into renewable gaseous fuels, as products of organic digestion. Nonetheless, development of new solutions is required to prevent further carbon dioxide emissions. The paper presents a novel dual approach developed to reduce carbon dioxide emissions from stationary power units, basing on spark ignition engine. The discussed approach includes both reduction in carbon content in the fuel, which is realized by its enrichment with hydrogen produced using the solar energy-supported electrolysis process, as well as application of post-combustion carbon dioxide separation. Results of the performed analysis suggest profitability of transition from fossil into the hydrogen-enriched fuel mixture, with significant rise in operational parameters of the system following increase in the hydrogen content. Nevertheless, utilization of the carbon dioxide separation leads to vital soar in internal energy demand, causing vital loss in operational and economical parameters of the analyzed system.

Keywords: Spark ignition engines; Digestion gas cofiring; CO₂ emissions; Membrane separation

*Corresponding Author. Email: katarzyna.janusz-szymanska@polsl.pl

Nomenclature

c_{N_2}	–	nitrogen concentration in ambient air (oxidizer)
c_{O_2}	–	oxygen concentration in ambient air (oxidizer)
HC	–	hydrogen to carbon ratio (of the fuel)
\dot{n}_{CO_2}	–	molar stream of CO ₂ , kmol/s
\dot{n}_{H_2O}	–	molar stream of water vapor, kmol/s
\dot{n}_{CO}	–	molar stream of carbon monoxide, kmol/s
\dot{n}_{H_2}	–	molar stream of unburned hydrogen radicals, kmol/s
\dot{n}_{N_2}	–	molar stream of nitrogen, kmol/s
LHV	–	lower heating value
p_{BDC}	–	pressure inside the combustion chamber at the bottom dead center, MPa
p_{EVO}	–	pressure inside the combustion chamber at the exhaust valve opening, MPa
T_{Ex}	–	mean exhaust gas temperature, K
T_{EVO}	–	temperature of gases in combustion chamber at exhaust valve opening, K
T_{MCT}	–	mean temperature of combustion, K
γ_{Ex}	–	ratio of specific heats of the exhaust gas
λ	–	air to fuel ratio

Abbreviations

CHP	–	combined heat and power
CCHP	–	combined cooling, heat and power
DNI	–	direct normal irradiance
ICE	–	internal combustion engine
PIL	–	poly(ionic) liquid membrane
PIM	–	polymer membrane
PV	–	photovoltaic (module/system)
SI	–	spark ignition (engine)

1 Introduction

Protection of natural environment is one of the vital tasks faced by engineers. The continuous emission of number of chemical compounds to the atmosphere, soil and water crucially influences the state of our environment by limiting ability of its natural regeneration. Exploitation of non-renewable energy sources (as fossil fuels) and raw materials leads to their depletion. Therefore, replacing fossil fuels with alternative energy carriers from different sources seems to be essential. Thus, addition or even full replacement of conventional fuels by fuel mixtures, including those based on biogas and biomethane (fuels from anaerobic digestion of organic compounds) is considered as beneficial [1–3]. Hydrogen (H₂) – especially originating from the electrolysis process powered by renewable solar or wind energy – is also recognized as a promising energy carrier for fuel mixtures [4–6]. Although hydrogen is primarily considered as an energy carrier for fuel cells, it might

be applied as a fuel additive for internal combustion engines as well [7–13]. Since hydrogen is deemed as a ‘clean fuel’, partial replacement of fossils by hydrogen limits the emission of harmful substances (as hydrocarbons resulting from imperfect combustion) into the atmosphere and save natural resources.

Furthermore, individual units and distributed generation systems are deemed to be appropriate to ensure better coverage of the energy demand of local consumers [14]. Reduction of primary fuel consumption [15,16] and improvement in the energy efficiency might be acquired by simultaneous generation of electricity and heat/cold in small-scale facilities – also using renewable and/or conventional resources. Such combined systems – combined heat and power (CHP) and combined cooling, heat and power (CCHP) – enable reduction of the emission of greenhouse gases to the atmosphere, when compared to separated systems. Regarding the small-scale units, especially belonging to the group of CHP/CCHP systems, commonly utilize the spark ignition engines (SI). In recently performed research, reductions of emissions coming from such units, especially considering carbon dioxide (CO₂) emissions, are recognized as the issue of particular importance.

Distributed energy systems, including individual units, often utilize internal combustion engines which can be fuelled with conventional (fossil) and alternative fuels (including products of digestion, as landfill gas or hydrogen) [3,7,10,12]. Nonetheless, selection of the proper internal combustion engine (ICE) or its adjustment for given system is influenced by many factors [7,17–20]. High methane share in derived fuel mixture is followed by, *i.e.* the increase in carbon monoxide/dioxide emissions, whereas rise in the hydrogen share results in increase in NO_x emissions [9,11], drop in CO₂ emissions [2,3] and higher water vapour content [3]. The proper combination of fossil and alternative fuels in a homogenous fuel mixture may provide an effective method to reduce emissions from individual unit. Nonetheless, to improve ecological characteristics, during transition from conventional to alternative fuel, internal combustion engines may require modifications in operational parameters, such as: adjustment of compression ratios [2], change of fuel-air ratio in the engine [11], modification of the cooling system [21] or integration with advanced exhaust gases treatment units [12].

Among variety of alternative fuels, suitable to be used as an additive to the fuel mixture derived to the ICEs, hydrogen gathered particular attention [22–24]. Its high energy per unit volume, resulting in visible change in combustion pressure, temperature and heat fluxes, without significant difference in timing of respective phases is recognized as the fundamental

reason [22,25]. Although currently the steam methane reforming is the most efficient and common method for industrial-scale hydrogen generation [26], its electrolytic generation gains focus as well [27,28] due to easy interconnection with renewable energy sources [27,29], even in the case of lacking method for its efficient storage and non-negligible losses in its transportation [30]. Due to low investment and maintenance expenditures as well as simple service, electrolysis performed in highly alkaline conditions is commonly used in market-available, low-power units [27,30].

Nonetheless, partial replacement of fossil fuel with its alternative equivalent might be not sufficient, regarding further reduction of CO₂ emissions from CHP systems with an internal combustion engine. To achieve the goal, membrane separations systems might be used. Depending on their particular application, membrane systems are able to separate CO₂ as well as SO₂, oxygen, nitrogen or hydrogen [31]. Basically, they are characterized by a simple, modular structure – which is deemed as their main advantage. Nevertheless, to ensure proper operation, the membrane separator must be properly selected for the separated gases [31,32]. Membranes are commonly sensitive to both temperature and pollution [32,33]. The large group of polymer membranes (PIM), including, *i.e.* polyimides, is very often used for CO₂ separation – nonetheless, water vapour is harmful for some of them [34–36]. Positive influence of water content in flue gas on CO₂ separation is shown by poly(ionic liquid) membranes (PIL), where the presence of water contributes to an 80% increase in CO₂ permeability through the membrane relative to dry gas [37,38]. Nevertheless, CO₂ permeability for currently available PIL materials is much lower than for polyimide membranes (PIM) – 33 Barrer in laboratory conditions for PIL to over 2000 Barrer for PIM [38].

Hence, due to the higher permeability of carbon dioxide, affecting purification of gases in CHP systems with an internal combustion engine, polymeric membranes seem to be the most appropriate.

The paper discusses the initial analysis of novel spark-ignition engine-based CHP system, supported with membrane separation unit CO₂ removal. The analysis focuses on investigation in operational and ecological parameters of the engine – including its power and CO₂ emissions – as well as thermal performance of the double-section heat exchanger system, inherently included within the simulated unit. Additionally, performance of the carbon removal unit, based on polyimide membrane, was investigated as well. Summary of the analysis was performed by fundamental recognition of

the hydrogen generation system, coupled with an independent renewable energy source (set of photovoltaic modules). The research was performed computationally, using the methodology of spark-ignition engine modelling discussed in reference [39] and basing on empirical dependencies acquired for market-available membrane gas separator [32]. Performance of the system was analyzed under variable composition of the fuel – enriched with the sewage-fermentation biogas and hydrogen as the potentially ecological substitutes for natural gas.

2 Materials and methods

The system, stating the matter of analysis, regards the simple configuration of the spark ignition engine-based CHP unit, equipped with basic CO₂ separation system. Scheme of its configuration is indicated in Fig. 1.

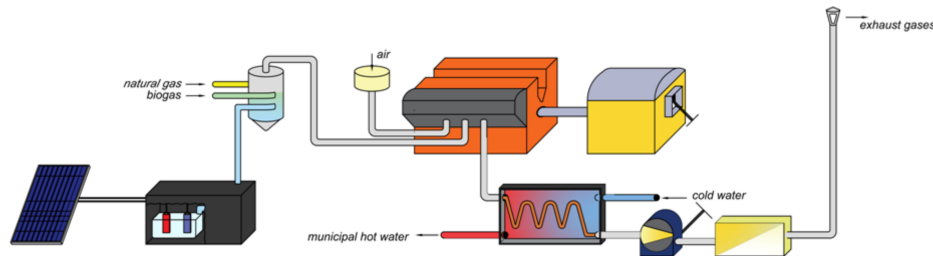


Figure 1: Scheme of the engine-based CHP unit with hydrogen generator and a membrane separator.

The investigation is performed using a simple mathematical model of the combined heat and power unit, equipped with J208 industrial spark ignition engine [41]. The model is prepared basing on the methodology of analysis described in [39] and discussed in details in [40]. The commercial Matlab computing software is selected as the main numerical environment for the analysis [52]. The model is coupled with a real gas model library, included within the professional general equation-solving software – Engineering Equation Solver (EES) [51], to determine respective heat fluxes and membrane separation unit performance. Brief data summary on the simulated engine is shown in Table 1.

Parameters of respective fuel mixtures derived into the engine, including primarily: composition, lower heating value (LHV), stoichiometric air-to-fuel ratio and averaged hydrogen-to-carbon ratio were calculated on the

Table 1: Selected data on J208 spark ignition engine manufactured by INNIO/GE Jenbacher (based on [41]).

Parameter	Value
Cylinder stroke, mm	145
Cylinder bore, mm	135
Compression ratio, –	9
Number of revolutions per power stroke, –	4
Number of cylinders, –	8
Rotational speed at nominal conditions, rev/min	1500

basis of experimental data, concerning composition and properties of respective fuels [42, 43], as well as the internal library included within the utilized EES computational environment. This software was also used to estimate the carbon footprint due to easy integration with the engine simulation software. This selection introduced significant simplification, regarding the carbon footprint calculations (i.e., ISO14067:2018 norm), nonetheless, vitally reducing length of the algorithm and computational cost. As the primary (reference) fuel for the simulated engine, the low-pressure natural gas of type E (high methane content), distributed within Polish gas network, was assumed [43]. The alternative fuels, used in variable individual shares to produce the final mixtures, regarded the biogas, resulting from natural fermentation process [42], and the hydrogen.

Due to high purity of the generated fuel, affordability and relatively wide market availability of ready-to-use equipment [27, 28, 44], the hydrogen was assumed to be produced during the water electrolysis process in an alkaline hydrogen generator. Temporary operational properties of the H₂ generator were simulated on the basis of experimental investigation, described in detail in references [27, 45]. The performed simulation was based on the hydrogen stream flow *vs.* derived electric power curve, obtained by applying the least squares approximation method on the experimental data [27, 45]. The key factor, influencing the applicability of the selected data, was the sizing of the hydrogen generation unit coupled with the modelled spark-ignition (SI) engine [29, 30, 44]. Thus, identification of the required hydrogen stream flow, calculated as the product of required stream flow of the fuel mixture derived to the engine and the hydrogen content within, had to be obtained first. Hence, the computational algorithm included estimation of operational parameters of the engine in the first step, and computation of the required electric power derived to the fuel generating unit in the next one.

In order to increase share of the renewable energy, utilized within the discussed system, additional coupling of the hydrogen generation unit with solar photovoltaic (PV) system was assumed. The considered solar system, including serial and parallel connection of monocrystalline silica cells of total max rated powers of 25 kWp and 1 MWp, respectively, was selected on the basis of high efficiency and ease direct connection to the hydrogen production unit [30, 45]. Performance of the photovoltaic system was estimated on the time span of one year, using the monthly-averaged direct normal (solar) irradiance (DNI) data, obtained using the PVGIS-CMSAF model (photovoltaic geographical information system – climate monitoring satellite application facility) for assumed location of the biogas source in Tychy (a city in Silesia Region, Poland). The selection of the radiation data source was based on its particularly low inaccuracy for long-time averaged data [46–48].

The engine model, which is the core of performed simulation, includes simplified analysis of combustion – basing on two-zone approach with prediction of specific heat ratios – and heat transfer – basing on averaged surface area within the cylinder [39]. The model simulates compression and expansion strokes, under assumption of variable air to fuel ratio – dependent on fuel mixture composition – and parameters of air and exhaust fumes with increment in crank angle rotation from opening of the inlet valve up to the closing of exhaust valve, with increment of one degree. The model incorporates the Weibe function and the Annand method during the simulated combustion phase (transition from compression into expansion strokes), with calculation of temperature of the exhaust gases basing on polytropic correlations [39, 40]

$$T_{Ex} = T_{EVO} \left(\frac{p_{BDC}}{p_{EVO}} \right)^{\frac{\gamma_{Ex}-1}{\gamma_{Ex}}}. \quad (1)$$

The exhaust gases composition is calculated on the basis of molar streams of respective compounds, estimated using the atom balance, regarding the excess air coefficient [39, 40]:

$$\dot{n}_{CO_2} = \frac{4}{\lambda(4 + HC)} - \left[2K_s \frac{4}{\lambda(4 + HC)} \left(\frac{1}{\lambda} - 1 \right) \right], \quad (2a)$$

$$\dot{n}_{H_2O} = 2 \left(1 - \frac{4}{\lambda(4 + HC)} \right) + \left[2K_s \frac{4}{\lambda(4 + HC)} \left(\frac{1}{\lambda} - 1 \right) \right], \quad (2b)$$

$$\dot{n}_{CO} = 2K_s \frac{4}{\lambda(4 + HC)} \left(\frac{1}{\lambda} - 1 \right), \quad (2c)$$

$$\dot{n}_{\text{H}_2} = 2 \left(\frac{1}{\lambda} - 1 \right) - \left[2K_s \frac{4}{\lambda(4 + \text{HC})} \left(\frac{1}{\lambda} - 1 \right) \right], \quad (2d)$$

$$\dot{n}_{\text{N}_2} = \frac{c_{\text{N}_2}}{c_{\text{O}_2}}, \quad (2e)$$

where

$$K_s = \exp \left(2.743 - 1.761 \times 10^3 T_{MCT}^{-1} - 1.611 \times 10^6 T_{MCT}^{-2} + 2.803 \times 10^{-9} T_{MCT}^{-3} \right).$$

Respective heat fluxes, transferred from the exhaust gases within the double-section heat exchanger, were calculated on the basis of energy conservation equation and parameters of the district heating and domestic hot water, required by the network, discussed in [49]. As the district heating temperatures at the inlet and outlet of the network, the values of 90°C and 70°C, respectively, were assumed. Considering the domestic hot water network, the inlet and outlet temperatures were assumed at the levels of 10°C and 55°C, respectively. For both sections of the exchanger, the 5 K pinch was assumed.

The operational parameters of the membrane separation unit were based on estimated performance of four polyimide UBE UMS-A2 membranes, working in parallel and coupled with an ideal gas compressor of 90% isentropic efficiency. The dependence of the recovery coefficient of the assumed membrane on the feed stream flow and moisture content was calculated basing on empirical data, presented in [32].

3 Results and discussion

Brief summary of the first part of the analysis, concerning parameters of the engine set under variable fuel composition, is shown in Table 2.

As presented, in Table 2, change in composition of the fuel mixture vitally influences performance of the engine as well as parameters of the exhaust gases. Regarding the reference case of the unit fuelled with pure natural gas, total electric power output of 300 kW with primary energy efficiency of 38.79% was indicated. At this case, temperature of the exhausts at the outlet collector equals almost 634°C, with CO₂ content slightly exceeding 9% in moist gas. High humidity (19% H₂O content in moist) is also characteristic for this case. Increase in share of biogas in the fuel mixture leads to drop in the power output of the engine – for the 90% biogas share,

Table 2: Summary of results of the engine operation: NG – natural gas, B – biogas, H₂ – hydrogen.

Fuel mixture composition, %mol	Power, kW	Power generation efficiency, %	Exhaust gas temp., °C	Exhaust gas mass flow, kg/s	CO ₂ share (moist exhaust gas), %vol	Water vapor share (moist exhaust gas), %vol	CO ₂ emission factor, kgCO ₂ /kJ _e	Total primary energy use efficiency, –
100% NG	300.0	38.79	633.5	0.467	9.1	19.0	0.061	0.884
50% NG, 50% B	283.0	38.81	608.3	0.587	10.2	17.3	0.087	0.895
30% NG, 70% B	274.5	38.77	594.5	0.647	10.7	16.4	0.101	0.900
10% NG, 90% B	264.7	38.78	577.6	0.715	11.2	15.5	0.118	0.907
27% NG, 70% B, 3% H ₂	296.5	38.80	635.5	0.642	10.7	16.4	0.098	0.897
25% NG, 70% B, 5% H ₂	311.5	38.77	663.7	0.640	10.7	16.4	0.095	0.894
23% NG, 70% B, 7% H ₂	326.8	38.71	692.3	0.637	10.7	16.4	0.093	0.890
7% NG, 90% B, 3% H ₂	288.2	38.80	622.1	0.712	11.3	15.5	0.115	0.903
5% NG, 90% B, 5% H ₂	304.3	38.77	652.5	0.710	11.3	15.5	0.112	0.900
3% NG, 90% B, 7% H ₂	319.2	38.74	680.5	0.704	11.3	15.5	0.109	0.897

the unit generated 264.7 kW, consuming 682.6 kW of primary energy in the fuel. Volumetric flow of the exhaust gases was increased by over 53%, regarding the reference case (0.715 kg/s to the 0.467 kg/s, respectively), with significantly higher CO₂ share of 11.2% in moist gas. The reason for such observation is an exceptionally high content of CO₂ in the applied biogas, equal to 35% in dry fuel. Rise in both exhaust gas emission and CO₂ content lead to a vital soar in CO₂ emission factor, equal to 0.101 kgCO₂/kJ_e in 90% biogas case to 0.061 kgCO₂/kJ_e for the reference, respectively. Nevertheless, due to the higher heat flux introduced to the low-temperature

section of hot water heat exchanger, the total primary energy efficiency of the co-generating unit increases with rise in biogas content (from 0.884 for the reference case to 0.900 for the highest biogas share case). Essential change in operation of the system is visible for the fuel mixtures, including hydrogen. Considering the natural gas-rich mixture, 3% addition of hydrogen leads to rise in temperature of exhausts up to 635.5°C (2°C than for the pure natural gas case), with only 1.2% reduction of available electric power, comparing to the reference. Nevertheless, due to over 37% higher volumetric flow of exhaust gases, almost double rise in CO₂ emission factor is observed. Results of the analysis, regarding the exhaust gas parameters, are depicted in Figs. 2 and 3.

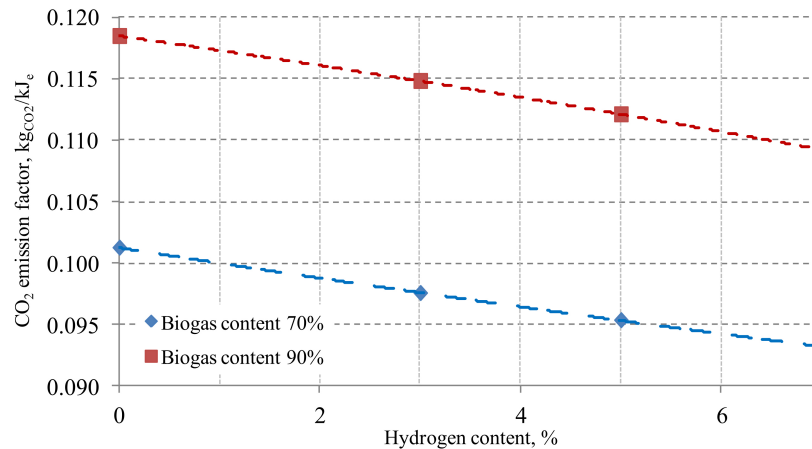


Figure 2: CO₂ emission factor as function of hydrogen share in the fuel for respective biogas contents.

As shown in Fig. 2, significant rise in CO₂ emissions occurs for 90% biogas content, proving vital importance of CO₂, carried by the fuel, within total CO₂ emissions. Nevertheless, independently on biogas content, the rise in hydrogen share in the fuel mixture was followed by a drop in CO₂ emission factor. As shown in Fig. 3, rise in the hydrogen content is followed by essential rise in exhaust gases temperature at the main collector's inlet. Regarding the biogas-lean mixture, partial replacement of natural gas with hydrogen in the initial fuel mixture leads to a rise in exhausts temperature up to 692°C (for the 7% hydrogen content). This essential change leads not only to higher potential of the central heating and domestic hot water production, but might vitally influence constructional features of re-

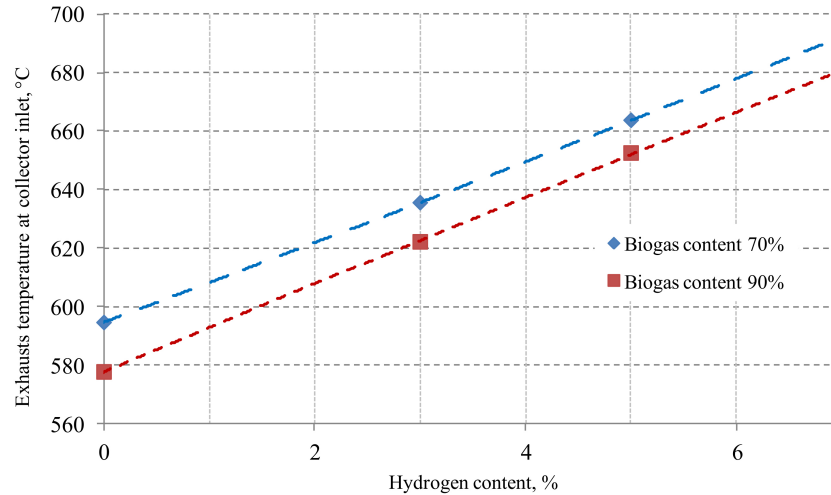


Figure 3: Temperature of exhaust gases (at inlet of the main outlet collector) as function of hydrogen share in the fuel for respective biogas contents.

spective heat exchangers and affect higher NO_x emissions. Lower exhaust temperatures, visible for the biogas-rich mixture, suggest influence of beneficial heat absorption of the triatomic CO_2 molecule, included within the biogas. Thus, the discussed results suggest, that there is optimal ratio of the hydrogen and biogas concentrations within the fuel mixture, enabling acquisition of low NO_x and CO_2 emissions with simultaneous significant rise in exhaust fumes temperature.

Results concerning the electric and thermal power outputs of the analyzed, engine-based CHP unit are shown in Fig. 4. Rise in hydrogen share in the fuel mixture leads both to rise in the electric and thermal power outputs, as indicated in Fig. 6. For both 70% and 90% shares of biogas in the fuel, linear dependence of generated power and heat with rise in hydrogen content is visible. Regarding the electric performance of the engine-based unit, for the 7% share in hydrogen, the unit generated 326.8 kW_e for the natural gas-rich and 319.2 kW_e for the natural gas-lean mixtures, respectively. This observation is in accordance with conclusion, regarding operation of the spark ignition engines, partially fuelled by hydrogen, discussed in [14]. Regarding the useful heat generation, the unit was characterized by 19.0% and 20.6% higher thermal outputs, for 70% and 90% biogas content, respectively. The discussed thermal power was transferred to the high-temperature section of heat exchanger, followed by a larger heat flux derived to the distributed

heating network. Furthermore, rise in the hydrogen content was directly correlated with a drop in CO₂ emission factor of max. 7.9% for the natural gas-rich and max. 7.6% for the natural gas-lean fuel mixtures, respectively.

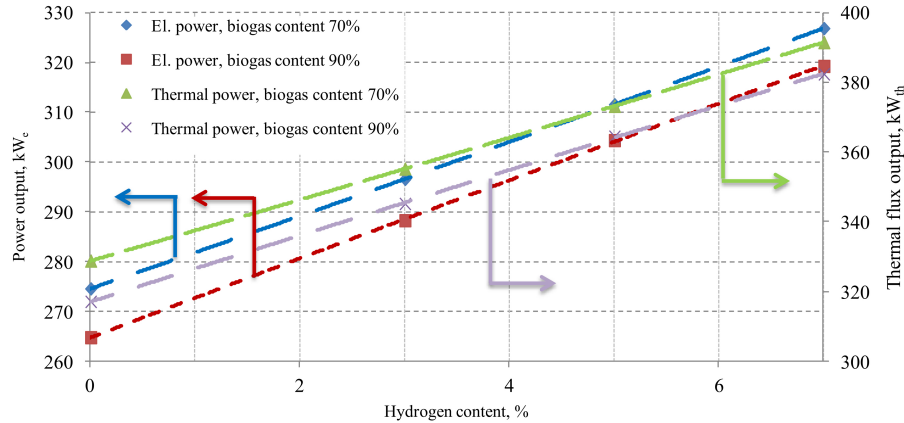


Figure 4: Output performance of the analyzed CHP system equipped with spark ignition engine.

Results of the investigation, concerning the membrane separation unit performance for respective cases, are summarized in Table 3.

As shown in the table, the rise in hydrogen content significantly affects the increase in water vapour flow within the exhaust gases. For the 70% biogas fuel case, the water vapour stream in exhausts was increased of up to 9.5%, whereas for the 90% biogas fuel, the water vapour flow was increased by up to 7.9%, in regard to the reference. Furthermore, despite the drop in CO₂ emissions coefficient, the total stream flow of emitted CO₂ soared with the rise in hydrogen content. Regarding the 70% biogas mixture, an up to 9.3% rise was observed, whereas for the 90% biogas mixture, a max increase of 11.3% was acquired. However, due to the rise in temperature of exhaust gases, no significant increase in humidity ratio, regarding respective reference cases, was observed. As shown by the recovery coefficient values, rise in the hydrogen share in the exhausts is followed by the rise in operational parameters of the membrane – which is caused by continuous drop in the exhausts stream flow. This observation suggests importance of adequate sizing of the membrane unit. Nevertheless, for all cases of biogas-enriched fuel mixture, the operational parameters of the CO₂ capturing membrane are lower than for pure natural gas used as a fuel. In the worst case scenario (corresponding to 90% biogas share with no hydrogen added), drop in

Table 3: Results of the membrane separation unit (MSU) part performance analysis: NG – natural gas, B – biogas, H₂ – hydrogen.

Fuel mixture composition, %mol	Water vapour mass flow in exhaust gas, kg/s	CO ₂ mass flow in exhaust gas, kg/s	Humidity ratio of exhaust gas	Recovery coefficient of the MSU, %
100% NG	0.023091	0.018	0.1493	41.1
50% NG, 50% B	0.025374	0.025	0.1332	31.9
30% NG, 70% B	0.025919	0.028	0.1249	28.6
10% NG, 90% B	0.026405	0.031	0.1168	25.7
27% NG, 70% B, 3% H ₂	0.026975	0.029	0.1249	30.0
25% NG, 70% B, 5% H ₂	0.027698	0.030	0.1249	31.0
23% NG, 70% B, 7% H ₂	0.028399	0.030	0.1249	32.0
7% NG, 90% B, 3% H ₂	0.027615	0.033	0.1168	26.9
5% NG, 90% B, 5% H ₂	0.028469	0.034	0.1168	27.7
3% NG, 90% B, 7% H ₂	0.029099	0.035	0.1168	28.6

the recovery coefficient approximates 27%. The total power demand of the membrane separation unit (MSU) – based on internal energy demand of the compressor – for all investigated cases was approximately equal to 113 kW.

In order to mitigate the negative influence of the CO₂ generated within the system, the effects of PV system incorporation were analyzed. The monthly-averaged direct normal irradiance (DNI) for the year of 2016, available for the PV system at the selected location (Tychy, Poland) is shown in Fig. 5. Data shows the peak irradiance available during the summer season, with the peak value of approx. 200 W/m² in June. Although the presented data might be deemed as inaccurate (i.e. due to neglecting the influence of indirect radiation), it follows the expected trend – considerable influence of coupling between the PV and SI systems on total power output shall occur between May and September, with no visible difference in autumn and winter seasons. The fundamental condition, regarding the available solar irradiance, is covering the demand for electrolytic hydrogen generation. The stream flow of the hydrogen, which has to be generated, depends on the mixture both due to variable concentration as well as changing fuel flow.

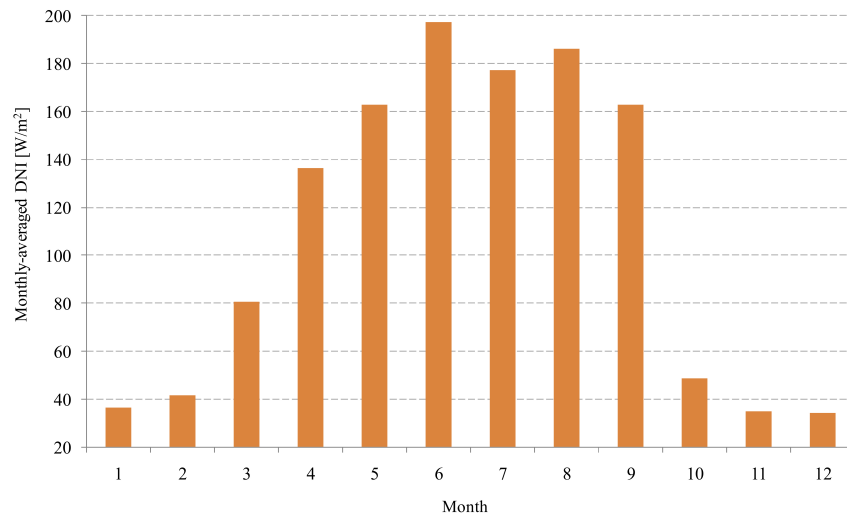


Figure 5: Monthly-averaged direct normal irradiance (DNI) at Tychy, Poland, for 2016 (data based on PVGIS-CMSAF model).

The average daily energy demand of the electrolytic hydrogen generator, depending on the fuel mixture being assumed, is shown in Fig. 6.

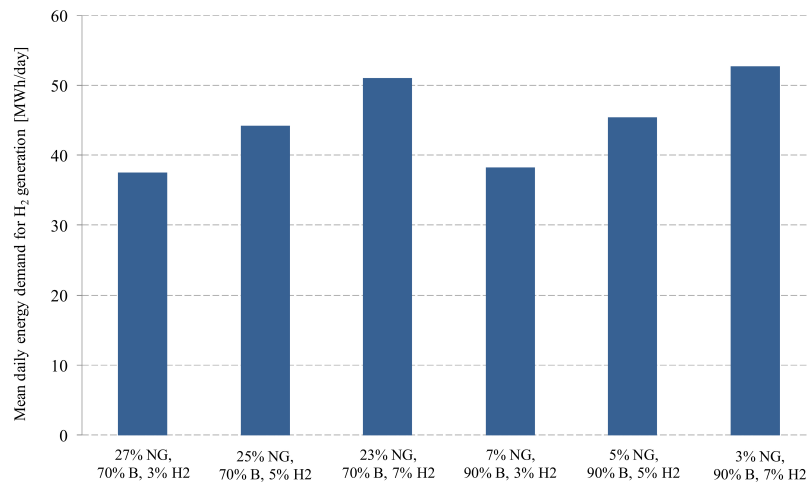


Figure 6: Average daily energy demand of the alkaline electrolytic hydrogen generator.

As indicated in Fig. 4, the internal power output from the modelled spark-ignition (SI) engine vitally depends on the applied fuel mixture. Considering

the contribution of the PV system and the stock market prices of electrical power, variable throughout the year [50], significant change in average incomes, following the change in the fuel and seasons is expected. Results of the simulation, regarding the change in expected profits for the PV-SI integrated system, operating with 25 kWp solar power and lacking the CO₂ separation, are shown in Fig. 7.

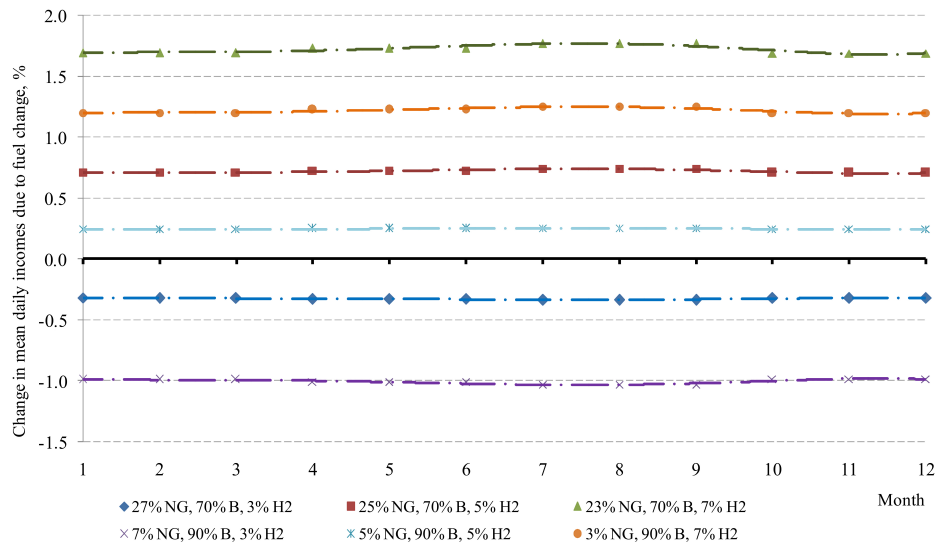


Figure 7: Relative change in daily-averaged incomes during the year, depending on the fuel mixture (for the PV-integrated system of 25 kWp output power).

Presented data clearly indicates essential dependence of incomes or losses on the applied fuel mixture. The highest rises in average daily income, equal to approximately 1.7% and 1.2%, are observed for highly hydrogen-enriched mixtures, including 7% of hydrogen content (with 70% and 90% of biogas, respectively). Among all investigated mixtures, application of two of them resulted in a year-long loss at the level of 0.4% (27% of natural gas) and 1.0% (7% of natural gas). This suggests, that when shifting towards ecological, low-calorific fuel, derivation of low amounts of highly-calorific fuel, combusting at high temperatures – as hydrogen – might be especially beneficial; nevertheless, utilization of too limited portions of hydrogen leads to permanent loss of its potential in mixture with CO₂-rich primary fuel. Further, incomes are partially influenced by the seasons – both the highest temporal rise in incomes (1.77%) and drop in losses (1.03%) are observed for the summer, when the solar irradiance and the national energy prices

are the highest. Selected results, regarding the analogical investigation performed for the larger PV system, are indicated in Table 4.

Table 4: Comparison of relative change in incomes due to fuel change for the SI system integrated with PV systems of 25 kWp and 1 MWp.

Month	Change in income for SI-PV integrated unit fuelled with 23% NG, 70% B, 7% H ₂ mixture, with 25 kWp of PV field, %	Change in income for SI-PV integrated unit fuelled with 23% NG, 70% B, 7% H ₂ mixture, with 1 MWp of PV field, %	Change in income for SI-PV integrated unit fuelled with 7% NG, 90% B, 3% H ₂ mixture, with 25 kWp of PV field, %	Change in income for SI-PV integrated unit fuelled with 7% NG, 90% B, 3% H ₂ mixture, with 1 MWp of PV field, %
March	1.690	1.692	-0.989	-0.984
June	1.729	1.731	-1.011	-1.004
September	1.766	1.768	-1.033	-1.028
December	1.687	1.688	-0.987	-0.985

As shown, similar results were obtained for the integrated system, operating with 1 MWp solar power PV unit. This proves that the amount of energy produced by the analyzed spark ignition engine system (assuming its stable operation in a longer time) is much greater than the energy derived from medium-scaled solar PV systems in the intermediate climate zone. Furthermore, the power required by the hydrogen generator container is significantly lower than energy surplus generated due to rise in operational parameters of the SI. Thus, the energy effect of joining the PV installation with the SI-based system, working at the selected location, is rather negligible – at least when considering the combustion engine of 300 kW rated power.

The results change vitally, when considering not only the replacement of fossil fuel by its biomass-origin substitution, but also the carbon capturing. As shown in Table 3, utilization of CO₂-enriched fuel, as the considered biogas, directly influences essential rise in CO₂ share in exhaust fumes with simultaneous drop in separation process efficiency. Therefore, although utilization of biogas enables better utilization of hydrogen potential (due to ease of transfer of high-temperature heat, generated during the combustion), it might vitally influence the costs of separation process. Results of the analysis, regarding the change in average incomes/losses for the full system, equipped with the CO₂ capturing, are shown in Fig. 8.

As indicated by respective data series, in the case of separation-equipped system, introduction of alternative fuel mixture always leads to drop in

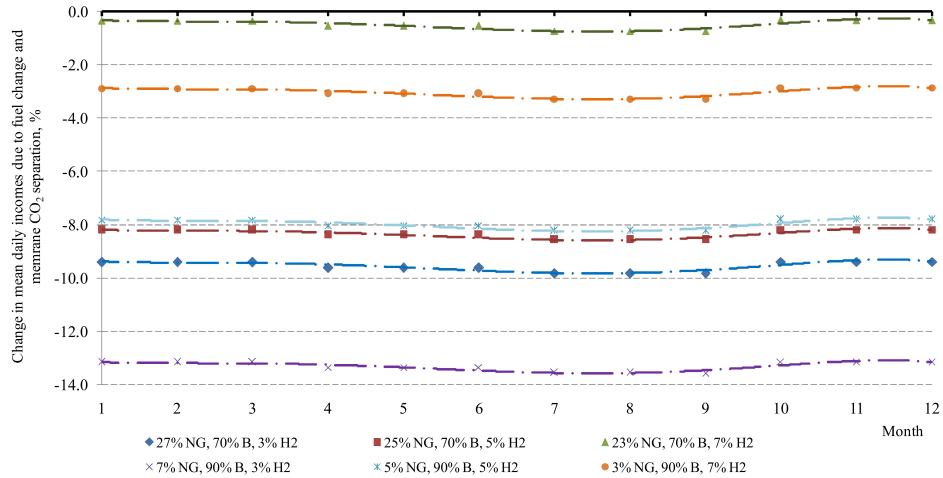


Figure 8: Relative change in daily-averaged incomes during the year, depending on the fuel mixture (for the PV-integrated system of 25 kWp output power), including the CO₂ separation expenses.

the incomes, varying in their average from 0.4% up to 13.6%. Again, the best results (the lowest loss) was observed for the 7%-hydrogen enriched mixtures. For all considered fuel mixtures, the losses increase in the summer season – what are caused by significant rise in the mean power prices. Similarly to the previous case, no vital difference was observed for the PV-SI integrated unit operated under 1 MWp – selected results of the analyses are compared in Table 5.

Table 5: Comparison of relative change in incomes due to fuel change for the SI system integrated with PV systems of 25 kWp and 1 MWp, including the expenses for CO₂ separation.

Month	Change in income for SI-PV integrated unit fuelled with 23% NG, 70% B, 7% H ₂ mixture, with 25 kWp of PV field, %	Change in income for SI-PV integrated unit fuelled with 23% NG, 70% B, 7% H ₂ mixture, with 1 MWp of PV field, %	Change in income for SI-PV integrated unit fuelled with 7% NG, 90% B, 3% H ₂ mixture, with 25 kWp of PV field, %	Change in income for SI-PV integrated unit fuelled with 7% NG, 90% B, 3% H ₂ mixture, with 1 MWp of PV field, %
March	-0.363	-13.181	-0.354	-13.171
June	-0.567	-13.384	-0.548	-13.366
September	-0.771	-13.589	-0.760	-13.578
December	-0.349	-13.166	-0.347	-13.164

As indicated above in considering the integrated system the differences in the output power from 25 kWp and 1 MWp systems influence the incomes to a small extent – the results deviate at the second or third decimal point. Thus, investing in larger photovoltaic farms to mitigate the costs of conventionally fuelled system is rather unjustifiable.

4 Conclusions

The research indicated beneficial influence of hydrogen addition into the natural gas/biogas fuel mixture for spark ignition engine-based power units. Depending on the concentrations of the biogas, hydrogen addition was followed by the rise in electric power, being generated, as well as significant increase in the heat flux transferred to the district heating exchanger. Nevertheless, due to significant rise in exhaust gases temperature, such solution might require prevention of the main outlet collector corrosion and higher NO_x emissions.

Application of sewage fermentation biogas-enriched fuel mixture leads to essential rise in CO₂ emissions, which is caused primarily by high CO₂ concentration within the fuel. Although this might introduce certain benefits, as drop in exhausts' temperature, this leads to a significant rise in total membrane separator load and drop in its operational parameters. Thus, considering the ecological parameters, excessive addition of pure sewage biogas might be deemed as disadvantageous. Nevertheless, the research suggests the presence of the optimal fuel mixture composition, influencing both satisfactory operational parameters of the power unit and low CO₂/NO_x emissions.

Energy demand of the hydrogen generation process is incomparably low to the potential rise in the energy produced by the unit, fuelled with hydrogen-enriched mixture. When considering the potential incomes, coming from utilization of the simplified system, profitability of transition from conventional to alternative fuel is visible for both 70% and 90% biogas content, but only for higher hydrogen shares (5% and 7%, respectively). Nonetheless, when considering the system operating with the membrane CO₂ separation unit, any change in fuel from pure natural gas is deemed as strongly unbeneficial due to large CO₂ content in the derived biogas.

Although utilization of all investigated fuel mixtures in the unit, equipped with CO₂ removal system, was followed by a loss in average daily

incomes (due to vital rise in internal energy demand of the SI unit), the loss indicated by the system supplied with 23% natural gas / 70% biogas / 7% hydrogen mixture is vitally lower, than for other cases. This suggests, that for similar mixture of intermediate natural gas content, lowered biogas share and increased hydrogen content, the investigated system might exhibit some profits.

Acknowledgements The scientific work is funded by the Silesian University of Technology within the framework of the statutory research fund no. 08/050/BK_21/0231. Authors kindly acknowledge contribution of Dr. Eng. Michał Jurczyk (Silesian University of Technology) during the electrolysis process assessment.

Received 25 February 2021

References

- [1] DA COSTA R.B.R. ET AL.: *Experimental investigation on the potential of biogas/ethanol dual-fuel spark-ignition engine for power generation: Combustion, performance and pollutant emission analysis*. Appl. Energ. **261**(2020), 114438.
- [2] AYAD S.M.M.E. ET AL.: *Analysis of performance parameters of an ethanol fueled spark ignition engine operating with hydrogen enrichment*. Int. J. Hydrogen Energ. **45**(2020), 8, 5588–5606.
- [3] CHŁOPEK Z.: *Ecological aspects of using bioethanol fuel to power combustion engines*. Eksploatacja i Niezawodność – Maint. Rel. **35**(2007), 3, 65–69.
- [4] KOTOWICZ J., WECEL D., JURCZYK M.: *Analysis of component operation in Power to Gas to Power operation*. Appl. Energ. **216**(2018), 45–59.
- [5] KOTOWICZ J., JURCZYK M.: *Economic analysis of an installation producing hydrogen through water electrolysis*. J. Power Technol. **99**(2019), 3, 170–175.
- [6] GUANDALINI G., ROBINIUS M., GRUBE T. CAMPANARI S., STOLTEN D.: *Long-term power-to-gas potential from wind and solar power: A country analysis for Italy*. Int. J. Hydrogen Energ. **42**(2017), 19, 13389–13406.
- [7] PAWANANONT K., LEEPHAKPREEDA T.: *Feasibility analysis of power generation from landfill gas by using internal combustion engine, organic Rankine cycle and Stirling engine of pilot experiments in Thailand*. Energy Proced. **138**(2017), 575–579.
- [8] LEACH F., KALGHATGI G., STONE R., MILES P.: *The scope for improving the efficiency and environmental impact of internal combustion engines*. Transport. Eng. **1**, (2020), 100005.
- [9] ORTIZ-IMEDIO R. ET AL.: *Comparative performance of coke oven gas, hydrogen and methane in a spark ignition engine*. Int. J. Hydrogen Energ. **13**(2020), 33, 17572–17586.

- [10] LEE J. ET AL.: *Effect of different excess air ratio values and spark advance timing on combustion and emission characteristics of hydrogen-fueled spark ignition engine*. Int. J. Hydrogen Energ. **44**(2019), 45 25021–25030.
- [11] ZHU H., DUAN J.: *Research on emission characteristics of hydrogen fuel internal combustion engine based on more detailed mechanism*. Int. J. Hydrogen Energ. **44**(2019), 11, 5592–5598.
- [12] DOBSLAW D., ENGESESSER K.-H., STORK H., GERL T.: *Low-cost process for emission abatement of biogas internal combustion engines*. J. Clean. Prod. **227**(2019), 1079–1092.
- [13] GAHLEITNER G.: *Hydrogen from renewable electricity: An international review of power-to-gas pilot plants for stationary applications*. Int. J. Hydrogen Energ. **38**(2013), 5, 2039–2061.
- [14] IRIMESCU A., VASIU G., TORDAI G.T.: *Performance and emissions of a small scale generator powered by a spark ignition engine with adaptive fuel injection control*. Appl. Energ. **121**(2014): 196–206.
- [15] BALAKHELI M.M. *et al.*: *Analysis of different arrangements of combined cooling, heating and power systems with internal combustion engine from energy, economic and environmental viewpoints*. Energ. Convers. Manage. **203**(2019), 112–253.
- [16] SHEYKHI M. *et al.*: *Performance investigation of a combined heat and power system with internal and external combustion engines*. Energ. Convers. Manage. **185**(2019), 291–303.
- [17] ARBABI P., ABBASSI ABBAS, MANSOORI Z., SEYFI M.: *Joint numerical-technical analysis and economical evaluation of applying small internal combustion engines in combined heat and power (CHP)*. Appl. Therm. Eng. **113**(2017), 694–704.
- [18] WU J., WANG J.: *Distributed Biomass Gasification Power generation system Based on Concentrated Solar Radiation*. Energy Proced. **158**(2019), 204–209.
- [19] PERKINS G.: *Techno-economic comparison of the levelised cost of electricity generation from solar PV and battery storage with solar PV and combustion of bio-crude using fast pyrolysis of biomass*. Energ. Convers. Manage. **171**(2018), 1573–1588.
- [20] GOSSLER H., DROST S., PORRAS S., SHIESSL R., MAAS U., DEUTSCHMANN O.: *The internal combustion engine as a CO₂ reformer*. Combust. Flame **207**(2019), 186–195.
- [21] BOVA S., CASTIGLIONE T., PICCIONE R., PIZZONIA F.: *A dynamic nucleate-boiling model for CO₂ reduction in internal combustion engines*. Appl. Energ. **143**(2015), 271–282.
- [22] CHO J., SONG S.: *Prediction of hydrogen-added combustion process in T-GDI engine using artificial neural network*. App. Therm. Eng. **181**(2020), 115974.
- [23] ZHU H., ZHANG Y., LIU F., WEI W.: *Effect of excess hydrogen on hydrogen fueled internal combustion engine under full load*. Int. J. Hydrogen Energ. **45**(2020), 39, 20419–20425.
- [24] SHULGA R.N., PUTILOVA I.V., SMIRNOVA T.S., IVANOVA N.S.: *Safe and waste-free technologies using hydrogen electric power generation*. Int. J. Hydrogen Energ. **45**(2020), 58, 34037–34047.

- [25] ESCOBAR-JIMENEZ R.F., CERVANTES-BOBADILLA M., GARCIA-MORALES J., GOMEZ AGUILAR J.F., HERNANDEZ PEREZ J.A., ALVAREZ-GALLEGOS A.: *Short communication: The effects of not controlling the hydrogen supplied to an internal combustion engine*. Int. J. Hydrogen Energ. **45**(2020), 29, 14991–14996.
- [26] DURAISWAMY K., CHELLAPPA A., SMITH G., LIU Y., LI M.: *Development of a high-efficiency hydrogen generator for fuel cells for distributed power generation*. Int. J. Hydrogen Energ. **35**(2010), 17, 8962–8969.
- [27] KOTOWICZ J., JURCZYK M., WECEL D.: *Analysis of hydrogn generator operation in alkali environment*. Rynek Energii **3**(2019), 60–66 (in Polish).
- [28] NIKOLIC M. V., TASIC G.S., MAKSIC A.D., SAPONJIC D.P., MIULOVIC S.M., KANINSKI M.P.M.: *Raising efficiency of hydrogen generation from alkaline water electrolysis – Energy saving*. Int. J. Hydrogen Energ. **35**(2010), 22, 12369–12373.
- [29] GIBSON T.L., KELLY N.A.: *Predicting efficiency of solar powered hydrogen generation using photovoltaic-electrolysis devices*. Int. J. Hydrogen Energ. **35**(2010), 3, 900–911.
- [30] WECEL D., OGULEWICZ W.: *Study on the possibility of use of photovoltaic cells for the supply of electrolyzers*. Arch. Thermodyn. **32**(2011), 4, 33–53.
- [31] STANOVSKY P. *et al.*: *Flue gas purification with membranes based on the polymer of intrinsic microporosity PIM-TMN-Trip*. Sep. Purif. Technol. **242**(2020), 116814.
- [32] WICIAK G.: *The influence of the moisture content in gaseous CO₂/N₂ mixture on selected parameters of CO₂ separation in a capillary polymeric membrane*. Desalin. Water Treat. **128**(2018), 314–323.
- [33] JASCHIK M., TAŃCZYK M., JASCHIK J., JANUSZ-CYGAN A.: *The performance of a hybrid VSA-membrane process for the capture of CO₂ from flue gas*. Int. J. Greenh. Gas Con. **97**(2020), 103037.
- [34] OLIVIERI L. ET AL.: *The effect of humidity on the CO₂/N₂ separation performance of copolymers based on hard polyimide segments and soft polymer chains: Experimental and modeling*. Green Energy Env. **1**(2016), 3, 201–210.
- [35] LASSEUGUETTE E., CARTA M., BRANDANI S., FERRARI M.-C.: *Effect of humidity and flue gas impurities on CO₂ permeation of a polymer of intrinsic microporosity for post-combustion capture*. Int. J. Greenh. Gas Con. **50**(2016), 93–99.
- [36] THEILER A., KARPENKO-JEREB L.: *Modelling of the mechanical durability of constrained Nafion membrane under humidity cycling*. Int. J. Hydrogen Energ. **40**(2015), 9773–9782.
- [37] NIKOLAIEVA D. *et al.*: *The performance of affordable and stable cellulose-based poly-ionic membranes in CO₂/N₂ and CO₂/CH₄ gas separation*. J. Membrane. Sci. **564**(2018), 552–561.
- [38] ANSALONI L. *et al.*: *Influence of water vapor on the gas permeability of polymeric ionic liquid membranes*. J. Membrane. Sci. **487**(2015), 199–208.
- [39] CUDDIHY J., BEYERLEIN S., WHITE T., CORDON D.: *MATLAB Modeling of an IC Engine as a Capstone Learning Experience in a Combustion Engines Course*. SAE Techn. Pap. 2016-01-0173, 2016.

- [40] BEYERLEIN S.: *MatLAB Engine Code: YZ250 Engine Model*. https://www.webpages.uidaho.edu/mindworks/ic_engines.htm (accessed 27 May 2020).
- [41] INNIO: Jenbacher type 2. Product datasheet, 2019. https://www.innio.com/images/medias/files/161/innio_br_t2_update_a4_en_2019_screen_ijb-119002-en.pdf (accessed 27 May 2020).
- [42] RUTKOWSKI K.: *Analysis of the efficiency and composition of biogas in a 1MW biogas power plant*. *Inżynieria Rolnicza* **131**(2011), 173–178 (in Polish).
- [43] Safety Data Sheet. Natural gas in transmission and distribution lines. PGNiG SA, Warsaw 2010 (in Polish).
- [44] BURTON N.A., PADILLA R.V., ROSE A., HABIBULLAH H.: *Increasing the efficiency of hydrogen production from solar powered water electrolysis*. *Renew. Sust. Energ. Rev.* **135** (2021), 110255
- [45] KOTOWICZ J., JURCZYK M., WECEL D., OGULEWICZ W.: *Analysis of hydrogen production in alkaline electrolyzers*. *J. Power Technol.* **96**(2016), 3, 149–156.
- [46] PSILOGLOU B.E., KAMBEZIDIS H.D., KASKAOUTIS D.G., KARAGIANNIS D., POLO J.M.: *Comparison between MRM simulations, CAMS and PVGIS databases with measured solar radiation components at the Methoni station, Greece*. *Renew. Energ.* **146**(2020), 1372–1391.
- [47] KAPLANI E., KAPLANIS S., MONDAL S.: *A spatiotemporal universal model for the prediction of the global solar radiation based on Fourier series and the site altitude*. *Renew. Energ.* **126**(2018), 933–942.
- [48] DONDARIYA C., PORWAL D., AWASTHI A., SHUKLA A.K., SUDHAKAR K. MURALI MANOHAR S.R., AMIT B.: *Performance simulation of grid-connected rooftop solar PV system for small households: A case study of Ujjain, India*. *Energ. Rep.* **4**(2018), 546–553.
- [49] Characteristics of Konin municipal heat energy enterprize (in Polish). <https://www.mpec.konin.pl/index.php/charakterystyka-systemu.html> (accessed 25 June 2020).
- [50] Information from the President of ERO (No. 22/2020) on the average selling price of electricity on the competitive market for 2019. Energy Regulatory Office, Warsaw, 30.03.2020 (in Polish). <https://www.ure.gov.pl/pl/urzad/informacje-ogolne/komunikaty-prezesa-ure/8794,Informacja-nr-222020.html> (accessed 25 June 2020).
- [51] EES – Engineering Equation Solver. F-Chart Software. <http://fchartsoftware.com/ees/> (accessed 15 May 2020).
- [52] MathWorks. https://www.mathworks.com/products/new_products/previous_release_overview.html (accessed 27 May 2020).